BIOCHEMISTRY
including biophysical chemistry & molecular biology

Article

pubs.acs.org/biochemistry

Kinetic Analysis of Lauric Acid Hydroxylation by Human Cytochrome P450 4A11

Donghak Kim,[†,‡] Gun-Su Cha,[§] Leslie D. Nagy,[†] Chul-Ho Yun,[§] and F. Peter Guengerich*[,†]

[†]Department of Biochemistry and Center in Molecular Toxicology, Vanderbilt University School of Medicine, Nashville, Tennessee 37232-0146, United States

[‡]Department of Biological Sciences, Konkuk University, Seoul 143-701, Republic of Korea

[§]School of Biological Sciences and Technology, Chonnam National University, Gwangju 500-757, Republic of Korea

Supporting Information

ABSTRACT: Cytochrome P450 (P450) 4A11 is the only functionally active subfamily 4A P450 in humans. P450 4A11 catalyzes mainly ω-hydroxylation of fatty acids in liver and kidney; this process is not a major degradative pathway, but at least one product, 20-hydroxyeicosatetraenoic acid, has important signaling properties. We studied catalysis by P450 4A11 and the issue of rate-limiting steps using lauric acid ω-hydroxylation, a prototypic substrate for this enzyme. Some individual reaction steps were studied using pre-steady-state kinetic approaches. Substrate and product binding and release were much faster than overall rates of catalysis. Reduction of ferric P450 4A11 (to ferrous) was rapid and not rate-limiting. Deuterium kinetic isotope effect (KIE) experiments yielded low but reproducible values (1.2−2) for 12-hydroxylation with 12-^{2}H-substituted lauric acid. However, considerable "metabolic switching" to 11-hydroxylation was observed with [12-$^{2}H_3$]lauric acid. Analysis of switching results [Jones, J. P., et al. (1986) *J. Am. Chem. Soc. 108*, 7074−7078] and the use of tritium KIE analysis with [12-^{3}H]lauric acid [Northrop, D. B. (1987) *Methods Enzymol. 87*, 607−625] both indicated a high intrinsic KIE (>10). Cytochrome b_5 (b_5) stimulated steady-state lauric acid ω-hydroxylation ~2-fold; the apoprotein was ineffective, indicating that electron transfer is involved in the b_5 enhancement. The rate of b_5 reoxidation was increased in the presence of ferrous P450 mixed with O_2. Collectively, the results indicate that both the transfer of an electron to the ferrous·O_2 complex and C−H bond-breaking limit the rate of P450 4A11 ω-oxidation.

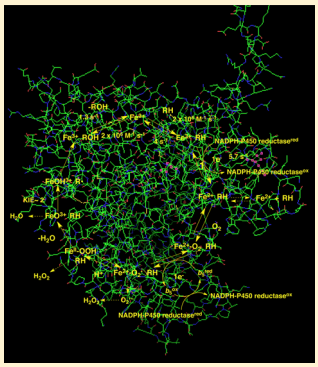

Cytochrome P450 (P450) subfamily 4A enzymes are historically important and also of considerable interest because of the biological activity of some of their products. Lauric acid 12-hydroxylation was the assay used in the first successful P450 solubilization/separation/reconstitution studies of Lu and Coon with rabbit liver microsomes.[1] Although what is known today as (rabbit) P450 2B4 was of the most interest in the subsequent efforts to first purify a mammalian P450,[2] our current knowledge base of catalytic specificity[3] would suggest that a P450 subfamily 4A enzyme might have been the object of the original study.[1] P450 4A subfamily enzymes have been studied extensively in several animal models and exhibit activity with a number of lipid substrates.[4−11] In humans, P450 4A11 appears to be the only subfamily 4A P450 enzyme, with the (*CYP*) 4A22 gene not encoding an active protein.[12]

The subfamily 4A P450s have several general properties in common. They use fatty acids and other long chain compounds as substrates.[13] Part of the heme becomes covalently attached in several, but this phenomenon does not appear to be linked to catalytic activity.[14,15] In contrast to several other P450s that oxidize fatty acids, many of the subfamily 4A P450s selectively catalyze ω-hydroxylation because of steric restriction in the active site.[16] No subfamily 4A P450 crystal structures are yet available, but some insight into structural features has been gleaned from site-directed mutagenesis.[16,17]

One of the more interesting translational aspects of (human) P450 4A11 research is the association of a single-nucleotide polymorphism (*rs1126742*) with an increased level of salt-sensitive hypertension.[18] The polymorphism has been associated with a 40% attenuation of arachidonic acid ω-hydroxylation activity because of the F434S amino acid substitution associated with the polymorphism.[18] The reaction product, 20-OH-eicosatetraenoic acid, has been shown to have both hypertensive and hypotensive properties in animal models.[19] The same reaction is also catalyzed by some human subfamily 4F P450s.[3,10]

Although there is considerable interest in P450 4A11 because of the biological properties of some of its products,[19−21] the amount of biochemical information about it is limited.[13,17,18,22] With recombinant P450 4A11 and the prototypic reaction of lauric acid 12-hydroxylation, varying (respective) k_{cat} and K_m values of 15 min^{-1} and 57 μM,[22] 38 min^{-1} and 200 μM,[17] and 20 min^{-1} and 11 μM,[18] respectively, have all been reported. Maximal activity is achieved in the presence of cytochrome b_5 (b_5).[17] Kawashima et al.[22] reported a lack of detectable arachidonic acid ω-hydroxylation activity by recombinant

Received: June 7, 2014
Revised: August 18, 2014
Published: September 9, 2014

dx.doi.org/10.1021/bi500710e | *Biochemistry* 2014, 53, 6161−6172

P450 4A11, but Gainer et al.[18] did find activity (k_{cat} = 2.2 min^{-1}), as we have in our own laboratory (with parameters similar to those of Gainer et al.,[22] unpublished results).

Despite the interest in P450 4A11 and its catalytic activities, very little is known about which step(s) in the catalytic cycle (Figure 1) limits activity. Studies with other human and

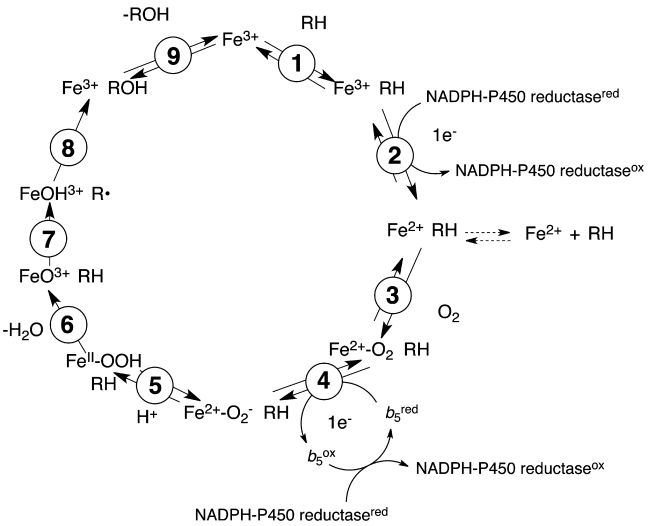

Figure 1. General catalytic P450 scheme.

experimental animal P450s have shown that steps 2, 4, 7, and 9 can all be rate-limiting in different reactions.[23,24] We utilized the approach of analyzing rates of individual reaction steps and measuring KIEs to kinetic models to determine which steps might be limiting, as has been done with several other P450s.[23,25−27] We conclude that major factors limiting the rate of lauric acid 12-hydroxylation are the rate of transfer of an electron from b_5 and the rate of C−H bond breaking. The intrinsic KIE was attenuated in steady-state kinetic measurements because it is not the only rate-limiting step.

EXPERIMENTAL PROCEDURES

Chemicals. Lauric (dodecanoic) acid (d_0, d_3, and d_{23}) and 12-OH lauric acid were purchased from Sigma-Aldrich and used without further purification. Lauric acid labeled with only one isotopic atom (d_1 or t_1) was prepared by the reaction of 12-bromododecanoic acid with NaB^2H_4 or NaB^3H_4, respectively, in $(CH_3)_2SO$.[28] The d_1 (^2H) reaction was conducted on a 10 mmol scale and the t_1 (^3H) reaction on a 0.10 mmol scale (with 5 mCi of NaB^3H_4, American Radiolabeled Chemicals, St. Louis, MO), and the product was recrystallized from a C_2H_5OH/H_2O mixture. The yields for the two reactions were 78 and 87%, respectively; the atomic excess of d_1-lauric acid was 90%, and the specific radioactivity of t_1-lauric acid was 0.23 mCi/mmol. [1-^{14}C]Lauric acid was purchased from American Radiolabeled Chemicals. Other chemicals were of the highest commercially available grade.

Enzymes. P450 4A11 was expressed in *Escherichia coli* from a pCW4A11 plasmid including a $(His)_6$ tag at the C-terminus. Expression and purification of P450 4A11 were conducted as previously described, with some modifications.[18,29] Briefly, the *E. coli* strain transformed with the pCW(Ori$^+$) vector was inoculated into Terrific Broth (TB) medium containing 100 μg mL^{-1} ampicillin and 1.0 mM isopropyl β-D-1-thiogalactopyranoside. The expression cultures (1 L) were grown at 37 °C for 3 h and then at 28 °C while being shaken at 200 rpm for 48 h in 2.8 L Fernbach flasks. The bacterial inner membrane fraction containing P450 4A11 was isolated and prepared from TB expression cultures using ultracentrifugation (10^5g for 60 min). The prepared membrane fraction was solubilized overnight at 4 °C in 100 mM potassium phosphate buffer (pH 7.4) containing 20% (v/v) glycerol, 0.1 mM EDTA, 10 mM β-mercaptoethanol, and 2% (w/v) 3-[(3-cholamidopropyl)dimethylammonio]-2-hydroxy-1-propanesulfonate (CHAPS) (Anatrace, Maumee, OH). The solubilized fraction, following ultracentrifugation (10^5g for 60 min), was then loaded onto a Ni^{2+}-nitrilotriacetate column (Qiagen, Valencia, CA), and the proteins were eluted with a buffer containing 300 mM imidazole. The eluted fractions containing P450 4A11 were subsequently dialyzed at 4 °C against 100 mM potassium phosphate buffer (pH 7.4) containing 20% (v/v) glycerol and 0.1 mM EDTA. The protein preparations were >90% pure as judged by sodium dodecyl sulfate−polyacrylamide gel electrophoresis (data not presented).

Rat NADPH-P450 reductase[30] and human b_5[31] were expressed in *E. coli* and purified as described previously. Apo-b_5 was prepared from b_5 by acid-acetone extraction as described previously.[32,33] *Pseudomonas* sp. protocatechuate dioxygenase was purchased from Sigma-Aldrich. Microsomes were prepared form a mixture of 10 individual human liver samples (mixed on the basis of equal mass) using a general differential centrifugation procedure.[34] The source of the human liver tissue was the Nashville Regional Organ Procurement Agency (approved by the Institutional Review Board).

Enzymatic Assays. Typical incubations included 0.2 μM P450 4A11, 0.4 μM NADPH-P450 reductase, 0.4 μM b_5, 150 μM L-α-dilauroyl-*sn*-glycero-3-phosphocholine, 100 mM potassium phosphate buffer (pH 7.4), 1 mM dithiothreitol, and the indicated concentration of lauric acid (usually added as an aqueous solution of sodium laurate) in a final volume of 0.50 mL. b_5 was included because it stimulated the catalytic activity (Figure 2). Following temperature equilibration to 37 °C for 5

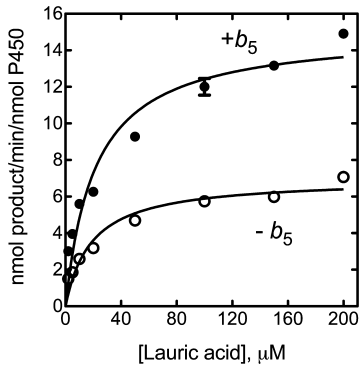

Figure 2. Effect of b_5 on lauric acid 12-hydroxylation activity of P450 4A11. Products were measured using the GC method, using a substrate concentration of 100 μM.

min, reactions were initiated by the addition of an NADPH-regenerating system consisting of 0.5 mM $NADP^+$, 10 mM glucose 6-phosphate, and 1 IU mL^{-1} yeast glucose 6-phosphate dehydrogenase.[34] Reactions generally proceeded at 37 °C for 15 min and were terminated with 1.0 mL of CH_2Cl_2 and the mixtures centrifuged (10^3g for 10 min). A 0.8 mL aliquot of the CH_2Cl_2 layer (lower phase) was transferred to a clean tube. An additional 1.0 mL of CH_2Cl_2 was added to the supernatant to

dx.doi.org/10.1021/bi500710e | *Biochemistry* 2014, 53, 6161−6172

extract the products, followed by centrifugation at $10^3 g$. The organic layers were combined, and the solvent was removed under a N_2 stream.

For GC−MS analysis, the dried extracts were converted to trimethylsilyl ethers by incubation with 50 μL of *N,O*-bis(trimethylsilyl)trifluoroacetamide containing trimethylchlorosilane [1% (v/v)] at 75 °C for 20 min [procedure based on BSTFA product specification/typical procedure provided by the supplier (Supelco/Sigma-Aldrich) (https://www.sigmaaldrich.com/content/dam/sigma-aldrich/docs/Supelco/Product_Information_Sheet/4746.pdf)]. The derivatized samples were allowed to cool, mixed using a vortex device, and transferred to sealed Teflon-capped glass vials for autoinjection on a Shimadzu GC-2010 gas chromatograph, using an Rtx-5 column [5% diphenyl/95% dimethylpolysiloxane capillary (w/w)] [30 m × 0.32 mm (inside diameter) × 0.25 μm (film thickness)], as previously described.[35] 10-Hydroxydecanoic acid was used as an internal standard. Hydroxylated products of lauric acid at the ω and ω-1 positions were identified by their characteristic mass fragmentation patterns. Turnover numbers of the hydroxylation of lauric acid at the ω and ω-1 positions by P450 4A11 were determined by a GC flame ionization detector (Shimadzu GC2010 instrument with a flame ionization detector). The distribution of products was based on the relative peak areas of the GC chromatograms (using 10-hydroxydecanoic acid as an internal standard). Similar rates were observed for GC−MS and the radioactive assays (*vide infra*).

In the case of reactions with human liver microsomes, the microsomes (1 mg of protein mL^{-1}) were used directly with the lauric acid substrates and the NADPH-generating system.

With 1-^{14}C-labeled lauric acid as a substrate, the dried extracts were dissolved in 100 μL of CH_3OH and then aliquots were analyzed on a reversed-phase (octadecylsilane, C_{18}) high-performance liquid chromatography (HPLC) column [5 μm, 2.1 mm × 100 mm (Waters, Milford, MA)] coupled with a radioisotope detector (IN/US Systems β-RAM, Tampa, FL). Reaction products and substrate were eluted at a flow rate of 0.6 mL min^{-1} using an increasing linear gradient of CH_3CN [including 0.1% (v/v) HCO_2H] from 40 to 95% (v/v) over 30 min.

Steady-state kinetic results were fit to hyperbolic plots in GraphPad Prism (GraphPad Software, San Diego, CA) to determine k_{cat} and K_m values, plus the standard error (SE) [see also Kinetic Isotope Effects (KIEs) (*vide infra*)].

Spectral Binding Titrations. Purified P450 4A11 was diluted to 2.0 μM in 0.10 M potassium phosphate buffer (pH 7.4), and binding spectra (350−500 nm) were recorded following subsequent additions of lauric acid or 12-OH lauric acid using an OLIS-Aminco DW2a spectrophotometer (Online Instrument Systems, Bogart, GA) as described previously.[36,37] The difference between the absorbance maximum and minimum was plotted versus the ligand concentration, and binding constants (K_d) and the SE were estimated using GraphPad Prism, either using either a hyperbolic fit or a quadratic equation.

Burst Kinetic Analysis. Burst kinetic analysis of lauric acid hydroxylation was conducted in a quench-flow apparatus (model RQF-3, KinTek Corp., State College, PA) as previously described.[38] P450 4A11 (100 pmol) was reconstituted as described above and incubated in the presence of 100 μM [1-^{14}C]lauric acid, in a total volume of 20 μL (per injection). Reactions were initiated by rapid mixing with 20 μL of 10 mM NADPH for a period of time ranging from 0.5 s to 4 min (as indicated) at 37 °C. Reactions were quenched with 300 μL of 3% (w/v) CCl_3CO_2H, and the production of 12-OH lauric acid was quantitated using HPLC as described for steady-state reactions.

Kinetic Isotope Effects (KIEs). *Noncompetitive (intermolecular) KIEs.* Noncompetitive (intermolecular) KIEs were measured by comparing k_{cat} and K_m values measured with d_0-, d_3-, and d_{23}-lauric acid as substrates, using the conventions of Northrop[39,40] for expressing KIEs as $^{D}V = {}^{H}k_{cat}/{}^{D}k_{cat}$ and $^{D}(V/K) = ({}^{H}k_{cat}/{}^{H}K_m)/({}^{D}k_{cat}/{}^{D}K_m)$. KIEs were measured for both 12- and 11-hydroxylation.

Competitive (intermolecular) KIEs. Competitive (intermolecular) KIEs were examined by incubating the P450 4A11 system with an equimolar mixture of d_0- and d_{23}-lauric acid (100 μM each) and measuring the relative amounts of 11- and 12-OH lauric acid formed by GC−MS. All four peaks were separated from each other because of the effect of the deuterium isotope on chromatography (t_R values of 16.5, 17.0, 19.0, and 19.4 min for d_{22}-11-OH lauric acid, d_0-11-OH lauric acid, d_{22}-12-OH lauric acid, and d_0-12-OH lauric acid, respectively).

Intramolecular (competitive) Deuterium KIEs. Intramolecular (competitive) deuterium KIEs were measured using d_1-lauric acid by LC−MS of the product 12-OH lauric acid, with the KIE being equal to 2 times the ratio of the intensities of the peaks at m/z 215 (d_0) and 216 (d_1), after correction for ^{13}C contributions[41] and the atomic excess of the d_1 substrate. (The statistical factor of 2 was used because all lauric acid molecules in the reaction have two C−H bonds and one C−D bond at C-12.)

An Intramolecular Tritium KIE. An intramolecular tritium KIE was estimated using t_1-lauric acid (0.23 mCi $mmol^{-1}$). Incubations with 100 μM t_1-lauric acid were terminated after 15 min at 37 °C via the addition of 50 μL of 6 M HCl. The aqueous reaction mixture was washed five times with 5 volumes of $(C_2H_5)_2O$. The radioactivity in the aqueous phase was measured using a liquid scintillation counter to estimate the amount of t-H_2O released, and the $(C_2H_5)_2O$ phase was evaporated to dryness. The residue was dissolved in CH_3CN, and an aliquot was used to measure tritium retention in 12-OH lauric acid by HPLC, using a radio-flow detector. The tritium KIE, $^{T}(V/K)$, was expressed as (disintegrations per minute of 12-OH lauric acid)/(disintegrations per minute of ^3H_2O) [because the protiated lauric acid is in a large excess of tritium and exchange of lauric acid with the enzyme is fast (*vide infra*), the competition is between the C−T bond and all of the C−H bonds in the lauric acid pool].

Intrinsic Deuterium KIE (^{D}k). The intrinsic deuterium KIE (^{D}k) was estimated from the deuterium and tritium KIE values using the approach of Northrop

$$[{}^{D}(V/K) - 1]/[{}^{T}(V/K) - 1] = ({}^{D}k - 1)/({}^{T}k - 1)$$

and the appropriate tables.[39]

Pre-Steady-State Kinetics. *General.* Pre-steady-state kinetic analysis was conducted using an OLIS RSM-1000 instrument (Online Instrument Systems, Bogart, GA), in the rapid-scanning absorbance mode. Typical conditions used 1.24 mm slits and 600-line, 300 nm gratings. The temperature was 37 °C in the case of the measurements involving substrate and product binding and reduction of ferric P450 4A11.

Substrate and Product Binding. One syringe contained 2.0 μM P450 4A11 in 100 mM potassium phosphate buffer (pH

dx.doi.org/10.1021/bi500710e | *Biochemistry* 2014, 53, 6161−6172

7.4); the other syringe contained 100 μM lauric acid or 12-OH lauric acid [added from a CH_3OH stock, final concentration of 0.5% (v/v) CH_3OH in 100 mM potassium phosphate buffer (pH 7.4)]. From the collected spectra, traces of ΔA_{390} and ΔA_{418} were fit to progress curves using DynaFit.[42]

Reduction of Ferric P450 4A11. Anaerobic tonometers[43−45] containing the reagents were used to load the stopped-flow syringes, which had been scoured overnight with a mixture of 1 mM protocatechuic acid and 0.03 unit mL^{-1} *Pseudomonas* sp. protocatechuate dioxygenase. The contents of the tonometers and syringes were under a CO atmosphere (positive pressure). One syringe contained 2 μM P450 4A11, 2.4 μM NADPH-P450 reductase, 60 μM L-α-dilauroyl-*sn*-glycero-3-phosphocholine, and (when indicated) 200 μM sodium laurate in 100 mM potassium phosphate buffer (pH 7.4). The other syringe contained 300 μM NADPH in 100 mM potassium phosphate buffer. Both syringes contained an oxygen scrubbing system composed of 1 unit mL^{-1} protocatechuate dioxygenase and 0.25 mM protocatechuate. Plots of decreases in A_{390} were used in that the ΔA_{450} rates were found to be slower because of an unexpectedly slow rate of CO binding (*vide infra*).

Oxidation of b_5. b_5 (3.0 μM) in 200 mM Tris-acetate buffer containing 75 μM L-α-dilauroyl-*sn*-glycero-3-phosphocholine, 10 mM EDTA, and 1 μM 5-deazaflavin[46] was photoreduced, as monitored in an OLIS-Cary 14 spectrophotometer (Online Instrument Systems) (2−3 min with a 500 W lamp positioned 15 cm away, immersed in a beaker of H_2O to prevent heating) and then transferred anaerobically to the stopped-flow spectrophotometer, where it was mixed with an equal volume of air-saturated 100 mM potassium phosphate buffer (pH 7.4). (The amines Tris and EDTA are sources of electrons.) Traces of ΔA_{409} and ΔA_{424} were fit to single-exponential plots.[26]

The experiment was repeated with 3.0 μM P450 4A11 or a mixture of 3.0 μM P450 4A11 and 3.0 μM b_5, in the presence of 1 mM tris(2-carboxyethyl)phosphine. Reduction was also conducted with 1 μM 5-deazaflavin and light (*vide supra*). Absorbance changes at 424 and 409 nm were used to estimate the rate of b_5 oxidation upon reaction of O_2 with ferrous P450 4A11.

Other Assays. NADPH oxidation rates were estimated by ΔA_{340} measurements using 0.15 μM NADPH (no generating system; $\Delta\varepsilon_{340}$ = 6.22 mM^{-1} cm^{-1}). Formation of H_2O_2 in reactions (500 μL) was initiated by adding 50 μL of 10 mM NADPH and terminated with the addition of 1.0 mL of CCl_3CO_2H [3% (w/v)] after 2 min. H_2O_2 concentrations were determined spectrophotometrically following reaction with ferroammonium sulfate and KSCN.[47] Reduction of O_2 to H_2O was estimated by a subtractive method described previously.[48]

Kinetic Fitting. DynaFit[42] was used to fit some of the kinetic and binding data, e.g., substrate and product binding (Supporting Information).

RESULTS

Reaction Stoichiometry. Lauric acid hydroxylation was demonstrated to be stimulated by b_5 (Figure 2 and Figure S1 of the Supporting Information). A similar dependence has been found for ω-hydroxylaiton of arachidonic acid with P450 4A11. Apo-b_5 was not effective (Figure S1 of the Supporting Information). Analysis of the overall reaction stoichiometry showed a pattern typical of mammalian P450s, with ∼30% of the electrons from NADPH used for hydroxylation of lauric acid (Table 1). All studies were conducted with 1 mM dithiothreitol or tris(2-carboxyethyl)phosphine present, in that these reductants (or glutathione) were consistently found to enhance catalytic activity 2−3-fold. The remainder of the reducing equivalents were used to reduce O_2 to H_2O_2 and H_2O[48] (Table 1).

Table 1. Stoichiometry of P450 4A11 Lauric Acid Hydroxylation[a]

reaction	rate (min^{-1})
NADPH oxidation	28 ± 1
lauric acid 12-hydroxylation	8.6 ± 0.5
H_2O_2 formation	13 ± 3
H_2O formation[b]	3 ± 1

[a]Results are presented as means ± the standard deviation (SD) (range) of duplicate assays. [b]H_2O formation was determined by calculating the difference between NADPH oxidized and the sum of H_2O_2 formation and products produced and then dividing by 2 (the SD for H_2O formation estimated from the square of sums of squares of individual SD values).[48]

To define the steps that limit the overall rate, we analyzed the rates of individual steps.

Substrate Binding (step 1 of Figure 1). 450 4A11, as isolated, is in a mixed iron spin state, mostly in the low-spin form; second-derivative analysis[49,50] indicated ∼10% high-spin iron. Addition of lauric acid is associated with a shift in the spin state to high spin ("type I").[36] The apparent K_d was 6.7 ± 0.3 μM. Fitting of the rate of the change (Figure 3) yielded an apparent k_{on} of 2 × 10^6 M^{-1} s^{-1} (1.2 × 10^8 M^{-1} min^{-1}) and a k_{off} of 4 s^{-1} (240 min^{-1}), assuming a two-state model (K_d = 2 μM). This k_{on} value is on the same order of magnitude of rate constants reported for P450 2A6,[26] much faster than seen for some other P450s for which productive binding probably involves multiple steps.[51,52]

Product Release (step 9 of Figure 1). Interaction of 12-OH lauric acid with P450 4A11 resulted in a shift of the basal high-spin iron component to a low-spin component, yielding a spectral change that was the opposite of that seen for the substrate lauric acid (or other fatty acids) and sometimes termed "reverse type I"[36] (Figure 4B). Titration with 12-OH lauric acid yielded an apparent K_d of 5.1 ± 2.1 μM (Figure 4D). Analysis of the kinetics of binding yielded an apparent k_{on} of 2 × 10^6 M^{-1} s^{-1} (1.2 × 10^8 M^{-1} min^{-1}) and a k_{off} of 1.3 s^{-1} (240 min^{-1}), assuming a two-state model. The k_{off} rate is much faster than the overall rate of catalysis (Table 1). An experiment designed to detect a possible burst reaction was clearly negative (Figure 5), indicating that a rate-determining step does not occur after product formation.

Reduction of Ferric P450 4A11. Ferric P450 4A11 was reduced by NADPH-P450 reductase in the presence of the substrate lauric acid (50 μM), under anaerobic conditions. The rates measured at 390 and 418 nm (decreased absorbance) represent the reduction of the high- and low-spin components, respectively, and were nearly identical [340 ± 10 and 280 ± 25 min^{-1}, respectively, for the fast phase (Figure 6)]. In both cases, a slower second phase (5 ± 1 and 6 ± 1 min^{-1}, respectively) followed.

P450 reduction experiments are usually monitored at 450 nm, recording the formation of the Fe^{2+}−CO complex. In this case (Figure 6), the kinetics of the fast phase (at 454 nm) were much slower than those measured at 390 or 418 nm, i.e., 48 ± 3 min^{-1}. This apparent discrepancy was shown to be due to an unexpectedly slow rate of CO binding (Figure 6D). At 50% (v/

dx.doi.org/10.1021/bi500710e | *Biochemistry* 2014, 53, 6161−6172

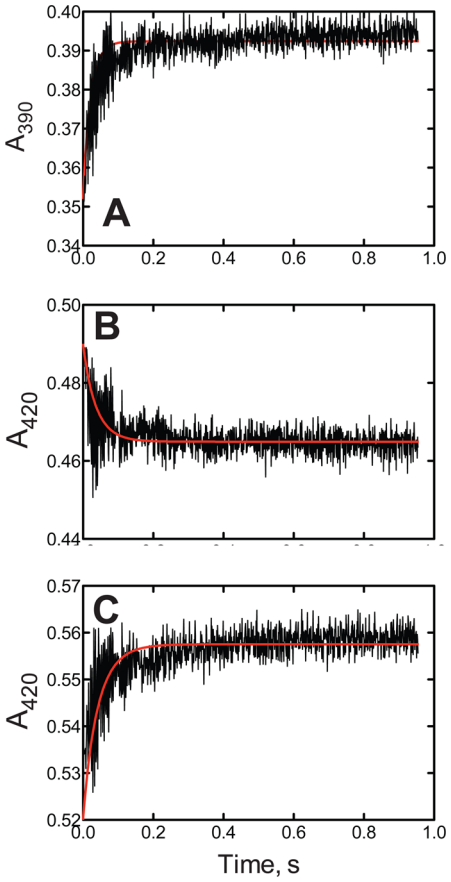

Figure 3. Rates of binding of lauric acid and 12-OH lauric acid to P450 4A11. The samples were mixed in a stopped-flow spectrophotometer as described in Experimental Procedures. Because of the low K_d values, estimates were made by fitting the reaction of 2 μM P450 4A11 and 2 μM ligand using DynaFit. Panels A and B show the changes in signals in opposite directions for the binding of lauric acid, and panel C shows the binding of 12-OH lauric acid. The red lines are fits to the rate constants that follow, using DynaFit (Supporting Information). (A and B) Lauric acid: k_{on} = 2 × 10 M^{-1} s^{-1} or 1.2 × 10^8 M^{-1} min^{-1}, and k_{off} = 4.0 s^{-1} or 240 min^{-1}. (B) 12-OH lauric acid: k_{on} = 2 × 10^6 M^{-1} s^{-1} or 1.2 × 10^8 M^{-1} min^{-1}, and k_{off} = 1.3 s^{-1} or 78 min^{-1}.

v) CO (nominal aqueous concentration of ~500 μM), the rate measured for the binding of CO was 66 min^{-1} (1.1 s^{-1}), corresponding to a second-order rate constant of ~2 × 10^3 M^{-1} s^{-1} (1.2 × 10^5 M^{-1} min^{-1}), much less than expected for a diffusion-controlled reaction. Other P450s have shown high rate constants; e.g., for P450 101A1, a reported rate constant is 5 × 10^6 M^{-1} s^{-1}, 50-fold higher.[53]

Transfer of the Second Electron to the P450 4A11 Fe^{2+}−O_2 Complex from b_5. P450 4A11 reactions are stimulated ~2-fold by b_5 (Figure 2), as reported previously by others.[17] Apo-b_5, devoid of heme, was not able to stimulate P450 4A11 lauric acid hydroxylation (Figure S1 of the Supporting Information). These results indicate that b_5 functions in this case by transferring an electron to the FeO_2^{2+} entity (Figure 1).

b_5 was photochemically reduced and mixed with air, being oxidized at a rate of 0.11 min^{-1} at 23 °C (data not shown). The experiment was repeated in the presence of photochemically reduced P450 4A11. A separate experiment with reduced P450 4A11 alone (reduction verified spectrally before introduction into the stopped-flow syringes) did not show a clear FeO_2^{2+}− complex spectrum. When the mixture of reduced P450 4A11 and b_5 was mixed with air, the b_5 was oxidized at a rate of 0.8 min^{-1} (at 23 °C), as judged by absorbance measurements at 390 and 424 nm (Figure 7). These studies indicate that the rate of b_5 electron transfer to the FeO_2^{2+} form of P450 4A11 is relatively slow (~1 min^{-1} at 23 °C), consistent with the modest enhancement (2-fold at 37 °C) of rates by b_5 (Figures 2 and 7).

C−H Bond Breaking and KIEs with Recombinant P450 4A11. One approach to judging the influence of the rate of C−H bond breaking on the overall reaction is the use of KIEs.[40,54,55] Preliminary KIE studies with d_0 and d_{23} (perdeutero) lauric acid suggested a relatively low KIE in noncompetitive (intermolecular) steady-state kinetic studies (Table 2). This was the case for both 12- and 11-hydroxylation (the latter accounting for <10% of the product).

More detailed studies were conducted with 12-d_3-lauric acid (Figure 8), in which C−H bonds are substituted with deuterium only at the major site of hydroxylation, i.e., C−H bond breakage. These experiments also yielded low KIEs in noncompetitive, intermolecular experiments (Table 2). Inverse KIEs (i.e., <1) were also observed for the minor product, 11-OH lauric acid (Table 2).

The low KIEs could be used to infer rapid C−H bond cleavage. However, the observed "metabolic switching"[56] (from 12- to 11-hydroxy product) is not consistent with this view. For a more appropriate analysis of the KIE, it is necessary to know the intrinsic KIE (^Dk) for C−H bond cleavage at carbon 12.

One approach to estimating ^Dk is with the use of an "isotopically sensitive branching" method, which can be applied when a minor product is also produced.[57,58] In the literature, this method has been applied to k_{cat} (^DV) results (actually applied to single-value results measured at high substrate concentrations).[57,58] With the knowledge that the reaction is irreversible and ignoring secondary KIEs, Jones et al.[58] transformed eq 1 (which is eq 10 of ref 57)

$$(k_H/k_D)_{obsd} = \frac{k_H/k_D + k_H/(k_{-1} + k_3)}{1 + k_H/(k_{-2} + k_3)}$$

into eq 2[58]

$$(k_H/k_D)_{obsd} = [k_H/k_D + (\text{ratio of primary C−H product})/(\text{secondary C−H product})]/[1 + (\text{ratio of primary C−H product})/(\text{secondary C−H product})]$$

which when transposed to the P450 4A11 system with the nomenclature used here gives

$$^DV = [^Dk + (\text{12-OH lauric acid})/(\text{11-OH lauric acid})]/[1 + (\text{12-OH lauric acid})/(\text{11-OH lauric acid})]$$

and in this case (Table 2) leads to

$$2.3 = (^Dk + 14.5/1.8)/(1 + 14.5/1.8)$$

and ^Dk = 13, the apparent intrinsic isotope effect, which is consistent with the large degree of metabolic switching (Table 2).

An alternate approach to estimating ^Dk comes from Northrop,[40] using noncompetitive intramolecular KIEs (V/K) and the relationship

dx.doi.org/10.1021/bi500710e | Biochemistry 2014, 53, 6161−6172

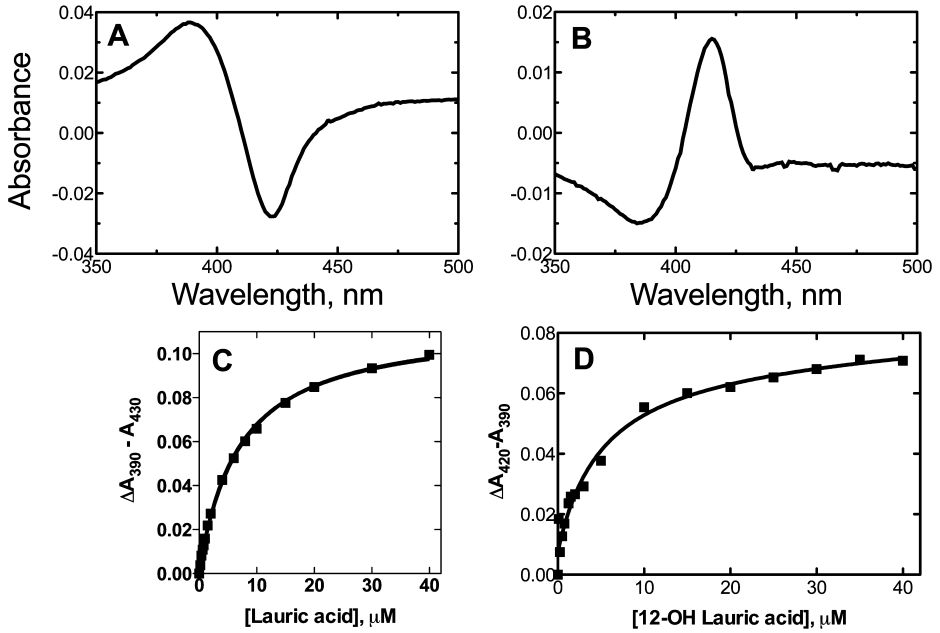

Figure 4. Binding of lauric acid and 12-OH lauric acid to P450 4A11. (A) Lauric acid. (B) 12-OH Lauric acid. The K_d values for (C) lauric acid and (D) 12-OH lauric acid were 6.7 ± 0.3 and 5.2 ± 2.1 μM, respectively. The binding parameters and SE were calculated from the single titrations shown in the plots, utilizing GraphPad Prism.

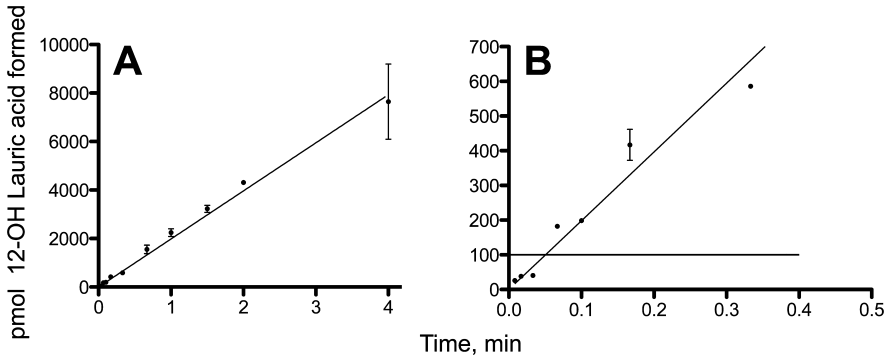

Figure 5. Lack of burst kinetics for P450 4A11-catalyzed ω-hydroxylation of lauric acid. The assays were conducted with 100 pmol of P450 at 37 °C. (A) Conventional steady-state kinetics. (B) A rapid quench apparatus was used for short time intervals. The resulting data points are fit to rates using linear regression analysis. The horizontal line in panel B (100 pmol of product, i.e., *y*-axis 100) is drawn to represent a single turnover of the enzyme.

$$[^{D}(V/K) - 1]/[^{T}(V/K) - 1] = (^{D}k - 1)/(^{T}k - 1)$$

using the nomenclature applied in this paper. We used MS analysis of the 12-OH lauric acid obtained from an incubation of 12-d_1-lauric acid to determine a $^{D}(V/K)$ value of 1.9 ± 0.1 (n = 3). 12-t_1-Lauric acid was prepared, and the ratio of tritium in the $^{3}H_2O$ (from cleavage of the C−T bond) and [^{3}H]-12-OH lauric acid (cleavage of the C−H bond, divided by 2 for statistical reasons) was used to calculate a $^{T}(V/K)$ of 3.5 ± 0.1 (n = 3). Solving the equation and using a set of tables,[39] $^{D}k \sim 20$ and $^{T}k \sim 77$ (with a 14% SE).

The overall conclusion is that the 12-hydroxylation reaction has a relatively high intrinsic KIE, ^{D}k, of 10−20, typical of a number of P450s.[23,25,59,60] The observed (noncompetitive) KIE is attenuated but still significant in the steady-state kinetic results.

Competitive (intermolecular) KIEs were measured using an equimolar mixture of d_0- and d_{23}-lauric acid. The KIE for 12-hydroxylation was 1.3 ± 0.2, and the KIE for 11-hydroxylation was 0.9 ± 0.1.

KIEs with Human Liver Microsomes. P450 4A11 is a major lauric acid ω-hydroxylase in liver microsomes, and we compared some of the KIE results, in this context of a more functional biological system. Only the work with d_0- and 12-d_3-lauric acid was done (Figure 9). As in the case of purified P450 4A11, 11-hydroxylation was a minor reaction. From the results obtained here, the following values were calculated for 12-hydroxylation: ^{D}V = 1.2 ± 0.2, and $^{D}(V/K)$ = 2.1 ± 0.7. For 11-hydroxylation, the values were as follows: ^{D}V = 1.0 ± 1.2, and $^{D}(V/K)$ = 0.15 ± 0.26. The high SEs in the 11-hydroxylation results are due to the low rates observed with the d_0 substrate, but the graph conveys the conclusion that the patterns (low KIE for 12-hydroxylation, strong metabolic switching to 11-hydroxylation) are similar to those with the purified enzyme system.

DISCUSSION

Although human P450 4A11 has been the subject of considerable interest because of its potential role in hypertension,[18] there is no crystal structure and relatively little work

dx.doi.org/10.1021/bi500710e | *Biochemistry* 2014, 53, 6161−6172

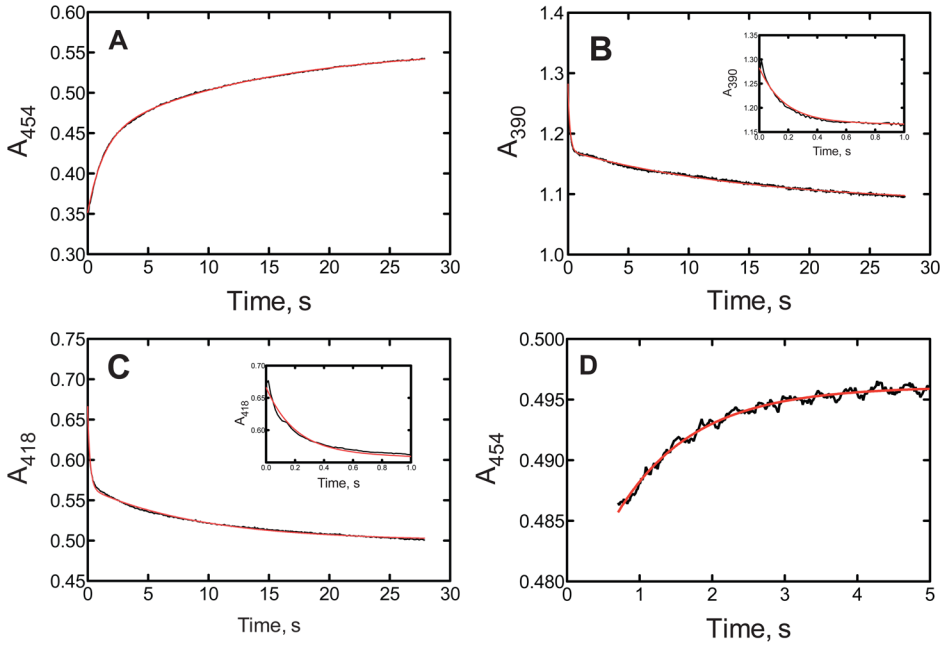

Figure 6. Reduction of ferric P450 4A11 and CO binding to Fe^{2+} P450 4A11. The samples were mixed in a stopped-flow spectrophotometer as described in Experimental Procedures. Traces are shown for reactions that included 100 μM lauric acid. The red lines show fits to the estimated rates, using the OLIS software (parallel first-order rates in panels A–C and pseudo-first-order rate in panel D). (A) The rates of the fast phase were 0.80 ± 0.05 s^{-1} and 48 ± 3 min^{-1} and of the slow phase 0.080 ± 0.01 s^{-1} and 4.8 ± 0.6 min^{-1}. (B) The rates of the fast phase were 5.7 ± 0.2 s^{-1} and 340 ± 10 min^{-1} and of the slow phase 0.080 ± 0.01 s^{-1} and 4.8 ± 0.6 min^{-1}. (C) The rates of the fast phase were 4.7 ± 0.4 s^{-1} and 280 ± 24 min^{-1} and of the slow phase 0.10 ± 0.02 s^{-1} and 6.0 ± 1.2 min^{-1}. (D) For binding of CO to Fe^{2+} P450 4A11, the rate was 1.1 ± 0.1 s^{-1} or 66 ± 7 min^{-1}.

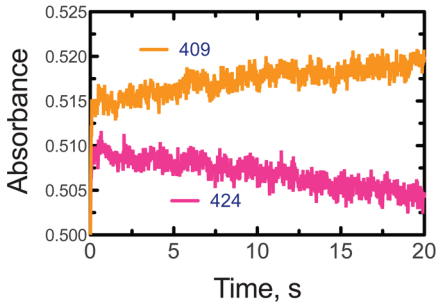

Figure 7. Reoxidation of ferrous b_5 in the presence of P450 4A11 Fe^{2+} and O_2. P450 4A11 (2.0 μM), in the presence of 75 μM L-α-dilauroyl-*sn*-glycero-3-phosphocholine, 1.0 mM tris(2-carboxyethyl)phosphine, 2.0 μM b_5, 100 μM lauric acid, and 1.0 μM 5-deazaflavin [in 200 mM Tris-acetate buffer (pH 7.4) containing 10 mM EDTA], was deoxygenated and then photoreduced (500 W lamp, 3 × 1 min) (verified using steady-state spectroscopy). The sample was introduced into the stopped-flow spectrophotometer and mixed with an equal volume of air-saturated 100 mM potassium phosphate buffer (23 °C). Analysis of the data yielded first-order rates of 0.079 ± 0.010 min^{-1} at 409 nm and 0.080 ± 0.013 min^{-1} at 424 nm. When the rate of reoxidation of photochemically reduced b_5 was analyzed under these conditions in the absence of P450 4A11, the reoxidation rate was 0.11 min^{-1} (data not shown).

has been published regarding its mechanism or, for that matter, any of the subfamily 4A P450s.[13,15,17,22] In this study, we considered a prototypic ω-hydroxylation reaction catalyzed by P450 4A11 and what steps are at least partially rate-limiting in catalysis. We conclude that at least two steps in the catalytic cycle, steps 4 and 7, contribute to the overall steady-state rate. Steps 1, 2, and 9 were shown to be rapid and because of this do not affect the overall rate.

The binding and release of ligands, at least the substrate and product, appear to be faster and simpler than in the case of some of the other human P450s, e.g., 3A4,[51,61] 1A2,[62] and 19A1.[52] These P450s appear to have more complex, multiphasic kinetics, and movement to the proximity of the iron is a slower, more complex process, which in some of the cases involves multiple ligands being present.[62,63] The differences may be due to the size of the active site, although this is still unknown in the case of P450 4A11. The fatty acid arachidonic acid is almost twice as long as lauric acid and is still a substrate.[18] It is possible that P450 4A11 has a much more rigid site, but this is also a matter of speculation. What is known is that subfamily 4A P450s have restricted active sites, which is somewhat intuitive as evidenced by their proclivity to oxidize terminal methyl groups, an energetically unfavorable reaction. Evidence of the oxygenation of even a chlorine atom positioned at the ω position has been presented.[16]

b_5 stimulates a number of P450s in an "allosteric" mode, instead of electron transfer.[64] One can speculate that b_5 may act in this mode because of its ability to bind and restrict motion of a flexible protein. P450s 2E1 and 2A6 also require electron transfer for the stimulatory effect of b_5,[26,64] and these enzymes are known to have relatively rigid, compact structures.[65,66]

The reduction of P450 4A11 is relatively rapid in the catalytic cycle (Figure 6). Binding of lauric acid clearly shifts the iron equilibrium toward the high-spin form (Figure 4). However, both high- and low-spin P450 4A11 iron showed similar rates of reduction by NADPH-P450 reductase (Figure 6). Although the view has been expressed that a shift in oxidation–reduction potential is associated with substrate binding and spin-state changes,[67] equivalent rates of reduction of high- and low-spin P450 iron have been shown here (Figure 6) and for P450 1A2.[45]

dx.doi.org/10.1021/bi500710e | *Biochemistry* 2014, 53, 6161–6172

Table 2. KIEs for Lauric Acid 12- and 11-Hydroxylation

lauric acid[a]	k_{cat} (min^{-1})	K_m (μM)	k_{cat}/K_m (μM^{-1} min^{-1})	^{D}V	$^{D}(V/K)$
			12-Hydroxylation		
d_0	12.1 ± 0.6	11 ± 2	1.1 ± 0.2		
d_{23}	8.4 ± 0.5	10 ± 2	0.9 ± 0.1	1.4 ± 0.1	1.3 ± 0.4
d_0	14.5 ± 0.7	19 ± 3	0.76 ± 0.12		
d_3	6.3 ± 0.1	10 ± 1	0.63 ± 0.06	2.3 ± 0.1	1.2 ± 0.2
			11-Hydroxylation		
d_0	0.77 ± 0.05	3.0 ± 1.0	0.25 ± 0.08		
d_{23}	0.55 ± 0.03	4.4 ± 1.0	0.13 ± 0.04	1.4 ± 0.1	2.0 ± 0.7
d_0	1.8 ± 0.2	27 ± 7	0.06 ± 0.02		
d_3	9.0 ± 0.3	16 ± 2	0.56 ± 0.07	0.18 ± 0.02	0.11 ± 0.04

[a]Products were measured using the GC method. The SE estimates are derived form within each hyperbolic fit of plots of the reaction rate (v) vs substrate concentration (S) in GraphPad Prism, and the SE in the quotients is the fractional square root of the sum of the fractional squares of the SE in both operators. The variation in the K_m values for 11-hydroxylation is attributed to the low rate for this reaction; e.g., see the plot for the microsomal reaction in Figure 9.

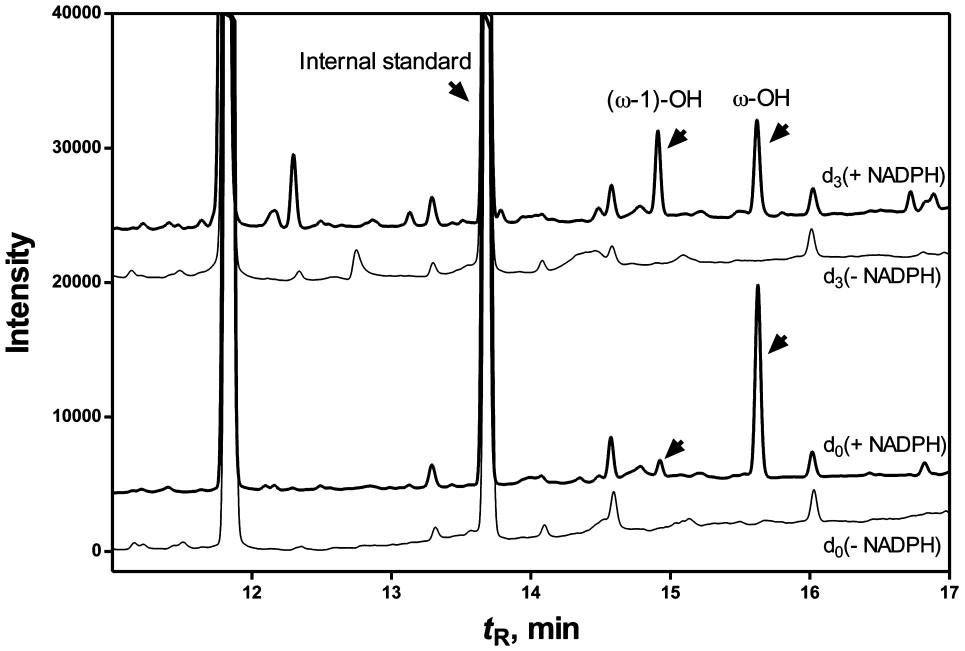

Figure 8. Effect of deuteration at carbon 12 on product distribution due to a KIE. The bottom traces show GC traces with d_0-lauric acid (with or without NADPH), and the top traces show the corresponding experiment with 12-d_3-lauric acid (100 μM in each case), with or without NADPH. The peaks identified as 11- and 12-OH lauric acid are designated with arrows, as is the internal standard 10-OH lauric acid.

The slow rate of CO binding (Figure 6D) was unexpected; we have not noticed this previously with other mammalian P450s.[26,33,45,52,68] The reason for the slow binding is unknown. Some plant P450s have low CO affinity,[69] but this is a case of a slow k_{on} rather than a fast k_{off}. There can be speculation about restricted access to the heme iron, based on the work with a rat orthologue.[66] One question that arises is whether O_2 access is also restricted. However, we were unable to detect an $Fe^{2+}-O_2$ complex in our work (Figure 7). If the rate of O_2 access were similar to that of CO (~60 min^{-1}), it would still be faster than overall turnover but could begin to contribute in that the overall rate of O_2 consumption is 28 min^{-1} for the enzyme (Table 1).

There has been considerable interest in identifying rate-limiting steps in P450 reactions since research in the field began.[70−72] KIEs were used in some early work,[70,71,73] although in many of these cases, it is not possible to interpret whether the finding of a significant primary KIE meant that C−H bond breaking contributed to a change in rate. Today there is no consensus regarding a single, unified rate-limiting step in all P450 reactions. However, in several cases, there is evidence that certain steps are limiting (this varies depending upon the experimental system and the particular oxidation reaction being studied). In the human P450 7A1-catalyzed 7α-hydroxylation of cholesterol, reduction of the ferric iron was concluded to be the most rate-limiting step.[27] With some P450s, there is evidence that b_5 stimulates reactions, and if apo-b_5 does not, then presumably b_5 is donating an electron to the $Fe^{2+}-O_2$ complex to facilitate the reaction (i.e., that step must be limiting).[64] This is the case with at least some of the catalyses of human P450 2A6[26] and 2E1.[64] With human P450 2E1 and the oxidation of ethanol, the most rate-limiting step follows product formation,[38,74] giving rise to burst kinetics and a KIE on K_m. For several P450s, high KIE values are observed in non-competitive experiments, e.g., P450s 1A2,[25] 2A6,[26] and 2D6,[75] indicative of major C−H bond breaking limitation on rates.

KIE studies can be complicated in that enzymatic reactions are complex and include multiple steps, only one of which is

dx.doi.org/10.1021/bi500710e | Biochemistry 2014, 53, 6161−6172

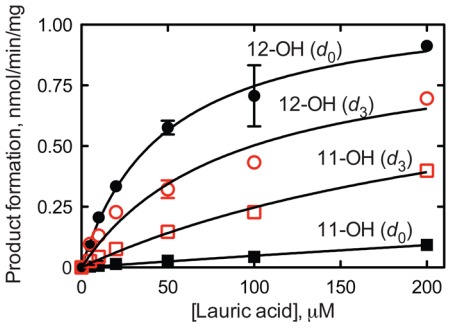

Figure 9. KIE patterns for lauric acid hydroxylation in human liver microsomes. The methods are described in Experimental Procedures. Assays were conducted in duplicate, and the points indicate the means ± the range. As described in Experimental Procedures, parameters were estimated using hyperbolic fits in GraphPad Prism, and SE values are from those fits. Rates are expressed on a milligram protein basis. The following parameters were obtained: for d_0 12-hydroxylation, V_{max} = 1.10 ± 0.06 nmol of product formed min^{-1} (mg of protein)$^{-1}$ and K_m = 48 ± 7 μM; for d_3 12-hydroxylation, V_{max} = 0.94 ± 0.11 nmol of product formed min^{-1} (mg of protein)$^{-1}$ and K_m = 86 ± 22 μM; for d_0 11-hydroxylation, V_{max} = 0.96 ± 1.18 nmol of product formed min^{-1} (mg of protein)$^{-1}$ and K_m = 1890 ± 2530 μM; for d_3 11-hydroxylation, V_{max} = 0.96 ± 0.12 nmol of product formed min^{-1} (mg of protein)$^{-1}$ and K_m = 288 ± 55 μM.

generally involved in C−H bond cleavage.[40,76] Two kinds of KIE measurements are particularly relevant for estimating the contribution of C−H bond cleavage to an overall reaction rate: (i) the intrinsic KIE (^Dk), which is an estimate for the KIE of the individual chemical C−H bond breaking step, and (ii) the noncompetitive intermolecular KIE, preferably $^D(V/K)$, which expresses the degree to which the ^Dk is expressed. A low $^D(V/K)$ value coupled with a high ^Dk indicates that C−H bond breaking is not a very rate-limiting step in the overall reaction.[77] While measurement of $^D(V/K)$ (and ^DV) (Table 2) is generally straightforward (if a suitable deuterated substrate is available), estimating ^Dk for a reaction may be more complex because of "masking" that results from "commitment to catalysis" and related factors.[77]

Two main approaches to estimating ^Dk have been used, the isotopically sensitivie branching method[57]and the tritium isotope method ("Northrop method").[39,40] The former can be applied when there is metabolic switching to an alternate product,[56] as in the case of ω-1 hydroxylation here (Figure 8). The Northrop approach requires the comparison of $^D(V/K)$ and $^T(V/K)$ with similarly labeled substrates, which is possible here through chemical synthesis, and had been previously applied to other P450 reactions.[60,78] Both approaches yielded high values for ^Dk, 13 and ∼20, respectively. These values may be compared with the low expressed values of ^DV and $^D(V/K)$ observed for ω-hydroxylation (1.2−2.3) in Table 2, indicating weak expression of a high intrinsic KIE. The situation is similar to that of P450 3A4-catalyzed testosterone 6β-hydoxylation, with a high ^Dk value established by Northrop's method but a low observed $^D(V/K)$.[60]

The concept of a relatively low KIE in typical experiments but a high intrinsic KIE is not novel, having been revealed by Miwa, Lu, and their associates with ethoxycoumarin reactions.[78] One question that can be asked is what the relationship is between the magnitude of a primary KIE (for a noncompetitive intermolecular comparison) and the contribution of a rate-limiting step.[23] The situation is complex with a P450 system, in that some of the steps (Figure 10) are reversible and there are also steps that result in the production of reduced and partially reduced oxygen species (Table 1). In previous work with another rabbit P450 1A2, kinetic modeling suggested that a KIE of 8.4 was related to an estimated 11-fold change in the rate of the C−H bond cleavage step due to deuteration,[25] but relating a smaller KIE to an actual ratio is more difficult. With the information available here, we can conclude that only step 7 (Figures 1 and 10) contributes at least partially to limiting rates of hydroxylation.

In conclusion, we have analyzed the P450 4A11 catalytic mechanism and found two steps that appear to be partly rate-limiting, steps 4 and 7 (Figure 10). Steps 1, 2, and 9 all appear to be too fast to be rate-limiting. We have not measured rates of steps 3, 5, 6, and 8, which are all more difficult or not even possible. Efforts to characterize a rate-limiting step by the

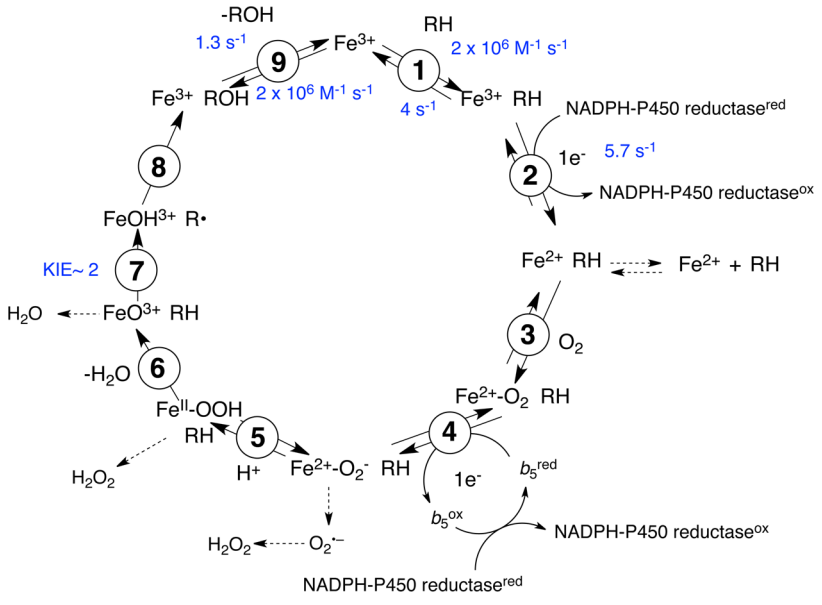

Figure 10. Generalized catalytic P450 scheme with measured rates or rate constants.

dx.doi.org/10.1021/bi500710e | *Biochemistry* 2014, 53, 6161−6172

nature of the accumulating spectral species in the steady state were unsuccessful because of the dominance of ferrous b_5 in the spectra (data not presented). Another point that should be made, in closing, is that the overall flux of the catalytic cycle (Figures 1 and 10) is a function of not only forward rates but also the leakiness of the system and abortive reduction of oxygen (Figure 10 and Table 1), which can undermine the catalytic efficiency of the system.

■ ASSOCIATED CONTENT

Supporting Information

DynaFit scripts and progress files for Figure 3 and effects of b_5 and apo-b_5 on catalytic activity. This material is available free of charge via the Internet at http://pubs.acs.org.

■ AUTHOR INFORMATION

Corresponding Author

*Department of Biochemistry, Vanderbilt University School of Medicine, 638 Robinson Research Building, 2200 Pierce Ave., Nashville, TN 37232-0146. E-mail: f.guengerich@vanderbilt.edu. Telephone: (615) 322-2261. Fax: (615) 322-4349.

Funding

This work was supported in part by National Institutes of Health Grants R37 CA090426 and P01 DK038226 (F.P.G.).

Notes

The authors declare no competing financial interest.
D.K. and G.-S.C. contributed equally to this work.

■ ACKNOWLEDGMENTS

We thank K. Trisler for assistance in preparation of the manuscript.

■ ABBREVIATIONS

b_5, cytochrome b_5; KIE, kinetic isotope effect; OH, hydroxy; P450, cytochrome P450.

■ REFERENCES

(1) Lu, A. Y. H., and Coon, M. J. (1968) Role of hemoprotein P-450 in fatty acid ω-hydroxylation in a soluble enzyme system from liver microsomes. *J. Biol. Chem. 243*, 1331−1332.

(2) Haugen, D. A., van der Hoeven, T. A., and Coon, M. J. (1975) Purified liver microsomal cytochrome P-450: Separation and characterization of multiple forms. *J. Biol. Chem. 250*, 3567−3570.

(3) Guengerich, F. P. (2005) Human cytochrome P450 enzymes. In *Cytochrome P450: Struture, Mechanism, and Biochemistry* (Ortiz de Montellano, P. R., Ed.) 3rd ed., pp 377−530, Kluwer Academic/Plenum Press, New York.

(4) Matsubara, S., Yamamoto, S., Sogawa, K., Yokotani, N., Fujii-Kuriyama, Y., Haniu, M., Shively, J. E., Gotoh, O., Kusunose, E., and Kusunose, M. (1987) cDNA cloning and inducible expression during pregnancy of the mRNA for rabbit pulmonary prostaglandin ω-hydroxylase (cytochrome $P\text{-}450_{p\text{-}2}$). *J. Biol. Chem. 262*, 13366−13371.

(5) Yoshimura, R., Kusunose, E., Yokotani, N., Yamamoto, S., Kubota, I., and Kusunose, M. (1990) Purification and characterization of two forms of fatty acid ω-hydroxylase cytochrome P-450 from rabbit kidney cortex microsomes. *J. Biochem. 108*, 544−548.

(6) Sawamura, A., Kusunose, E., Satouchi, K., and Kusunose, M. (1993) Catalytic properties of rabbit kidney fatty acid ω-hydroxylase cytochrome $P\text{-}450_{ka2}$ (CYP4A7). *Biochim. Biophys. Acta 1168*, 30−36.

(7) Aitken, A. E., Roman, L. J., Loughran, P. A., de la Garza, M., and Masters, B. S. S. (2001) Expressed CYP4A4 metabolism of prostaglandin E-1 and arachidonic acid. *Arch. Biochem. Biophys. 393*, 329−338.

(8) Hosny, G., Roman, L. J., Mostafa, M. H., and Masters, B. S. S. (1999) Unique properties of purified *Escherichia coli*-expressed constitutive cytochrome P450 4A5. *Arch. Biochem. Biophys. 366*, 199−206.

(9) Powell, P. K., Wolf, I., and Lasker, J. M. (1996) Identification of CYP4A11 as the major lauric acid ω-hydroxylase in human liver microsomes. *Arch. Biochem. Biophys. 335*, 219−226.

(10) Powell, P. K., Wolf, I., Jin, R., and Lasker, J. M. (1998) Metabolism of arachidonic acid to 20-hydroxy-5,8,11,14-eicosatetraenoic acid by P450 enzymes in human liver: Involvement of CYP4F2 and CYP4A11. *J. Pharmacol. Exp. Ther. 285*, 1327−1336.

(11) Cowart, L. A., Wei, S., Hsu, M. H., Johnson, E. F., Krishna, M. U., Falck, J. R., and Capdevila, J. H. (2002) The CYP4A isoforms hydroxylate epoxyeicosatrienoic acids to form high affinity peroxisome proliferator-activated receptor ligands. *J. Biol. Chem. 277*, 35105−35112.

(12) Bellamine, A., Wang, Y., Waterman, M. R., Gainer, J. V., III, Dawson, E. P., Brown, N. J., and Capdevila, J. H. (2003) Characterization of the CYP4A11 gene, a second CYP4A gene in humans. *Arch. Biochem. Biophys. 409*, 221−227.

(13) Hoch, U., Zhang, Z., Kroetz, D. L., and Ortiz de Montellano, P. R. (2000) Structural determination of the substrate specificities and regioselectivities of the rat and human fatty acid ω-hydroxylases. *Arch. Biochem. Biophys. 373*, 63−71.

(14) Hoch, U., and Ortiz de Montellano, P. R. (2001) Covalently linked heme in cytochrome P4504A fatty acid hydroxylases. *J. Biol. Chem. 276*, 11339−11346.

(15) LeBrun, L. A., Hoch, U., and Ortiz de Montellano, P. R. (2002) Autocatalytic mechanism and consequences of covalent heme attachment in the cytochrome P4504A family. *J. Biol. Chem. 277*, 12755−12761.

(16) He, X., Cryle, M. J., De Voss, J. J., and Ortiz de Montellano, P. R. (2005) Calibration of the channel that determines the ω-hydroxylation regiospecificity of cytochrome P4504A1: Catalytic oxidation of 12-halododecanoic acids. *J. Biol. Chem. 280*, 22697−22705.

(17) Dierks, E. A., Zhang, Z., Johnson, E. F., and Ortiz de Montellano, P. R. (1998) The catalytic site of cytochrome P450 4A11 (CYP4A11) and its L131F mutant. *J. Biol. Chem. 273*, 23055−23061.

(18) Gainer, J. V., Bellamine, A., Dawson, E. P., Womble, K. E., Grant, S. W., Wang, Y., Cupples, L. A., Guo, C. Y., Demissie, S., O'Donnell, C. J., Brown, N. J., Waterman, M. R., and Capdevila, J. H. (2005) Functional variant of CYP4A11 20-hydroxyeicosatetraenoic acid synthase is associated with essential hypertension. *Circulation 111*, 63−69.

(19) Roman, R. J. (2002) P-450 metabolites of arachidonic acid in the control of cardiovascular function. *Physiol. Rev. 82*, 131−185.

(20) Capdevila, J. H., Falck, J. R., and Harris, R. C. (2000) Cytochrome P450 and arachidonic acid bioactivation. Molecular and functional properties of the arachidonate monooxygenase. *J. Lipid Res. 41*, 163−181.

(21) Sävas, U., Machemer, D. E., Hsu, M. H., Gaynor, P., Lasker, J. M., Tukey, R. H., and Johnson, E. F. (2009) Opposing roles of peroxisome proliferator-activated receptor α and growth hormone in the regulation of CYP4A11 expression in a transgenic mouse model. *J. Biol. Chem. 284*, 16541−16552.

(22) Kawashima, H., Naganuma, T., Kusunose, E., Kono, T., Yasumoto, R., Sugimura, K., and Kishimoto, T. (2000) Human fatty acid ω-hydroxylase, *CYP4A11*: Determination of complete genomic sequence and characterization of purified recombinant protein. *Arch. Biochem. Biophys. 378*, 333−339.

(23) Guengerich, F. P. (2013) Kinetic deuterium isotope effects in cytochrome P450 reactions. *J. Labelled Compd. Radiopharm. 56*, 428−431.

(24) Guengerich, F. P. (2014) Experimental approaches to analysis of reactions of cytochrome P450 enzymes. In *Drug Metabolism Prediction* (Kirchmair, J., Ed.) Chapter 8, pp 199−219, Part 5 of Methods and Principles of Medicinal Chemistry (Kubinyl, H., Mannhold, R., and Folkkers, G., Series Eds.) Wiley-VCH, Weinheim, Germany.

(25) Guengerich, F. P., Krauser, J. A., and Johnson, W. W. (2004) Rate-limiting steps in oxidations catalyzed by rabbit cytochrome P450 1A2. *Biochemistry 43*, 10775−10788.
(26) Yun, C. H., Kim, K. H., Calcutt, M. W., and Guengerich, F. P. (2005) Kinetic analysis of oxidation of coumarins by human cytochrome P450 2A6. *J. Biol. Chem. 280*, 12279−12291.
(27) Shinkyo, R., and Guengerich, F. P. (2011) Cytochrome P450 7A1 cholesterol 7α-hydroxylation: Individual reaction steps in the catalytic cycle and rate-limiting ferric iron reduction. *J. Biol. Chem. 286*, 4632−4643.
(28) Bell, H. M., Vanderslice, C. W., and Spehar, A. (1969) The reduction of organic halogen compounds by sodium borohydride. *J. Org. Chem. 34*, 3923−3926.
(29) Kim, D., Wu, Z. L., and Guengerich, F. P. (2005) Analysis of coumarin 7-hydroxylation activity of cytochrome P450 2A6 using random mutagenesis. *J. Biol. Chem. 280*, 40319−40327.
(30) Hanna, I. H., Teiber, J. F., Kokones, K. L., and Hollenberg, P. F. (1998) Role of the alanine at position 363 of cytochrome P450 2B2 in influencing the NADPH- and hydroperoxide-supported activities. *Arch. Biochem. Biophys. 350*, 324−332.
(31) Guengerich, F. P. (2005) Reduction of cytochrome b_5 by NADPH-cytochrome P450 reductase. *Arch. Biochem. Biophys. 440*, 204−211.
(32) Cinti, D. L., and Ozols, J. (1975) Binding of homogeneous cytochrome b_5 to rat liver microsomes: Effect on N-demethylation reactions. *Biochim. Biophys. Acta 410*, 32−44.
(33) Yamazaki, H., Johnson, W. W., Ueng, Y.-F., Shimada, T., and Guengerich, F. P. (1996) Lack of electron transfer from cytochrome b_5 in stimulation of catalytic activities of cytochrome P450 3A4. Characterization of a reconstituted cytochrome P450 3A4/NADPH-cytochrome P450 reductase system and studies with apo-cytochrome b_5. *J. Biol. Chem. 271*, 27438−27444.
(34) Guengerich, F. P., and Bartleson, C. J. (2007) Analysis and characterization of enzymes and nucleic acids. In *Principles and Methods of Toxicology* (Hayes, A. W., Ed.) 5th ed., pp 1981−2048, CRC Press, Boca Raton, FL.
(35) Kim, D., Cryle, M. J., De Voss, J. J., and Ortiz de Montellano, P. R. (2007) Functional expression and characterization of cytochrome P450 52A21 from *Candida albicans*. *Arch. Biochem. Biophys. 464*, 213−220.
(36) Schenkman, J. B., Remmer, H., and Estabrook, R. W. (1967) Spectral studies of drug interaction with hepatic microsomal cytochrome P-450. *Mol. Pharmacol. 3*, 113−123.
(37) Shimada, T., Tanaka, K., Takenaka, S., Foroozesh, M. K., Murayama, N., Yamazaki, H., Guengerich, F. P., and Komori, M. (2009) Reverse type I binding spectra of human cytochrome P450 1B1 induced by flavonoid, stilbene, pyrene, naphthalene, phenanthrene, and biphenyl derivatives that inhibit catalytic activity: A structure-function relationship study. *Chem. Res. Toxicol. 22*, 1325−1333.
(38) Bell, L. C., and Guengerich, F. P. (1997) Oxidation kinetics of ethanol by human cytochrome P450 2E1. Rate-limiting product release accounts for effects of isotopic hydrogen substitution and cytochrome b_5 on steady-state kinetics. *J. Biol. Chem. 272*, 29643−29651.
(39) Northrop, D. B. (1977) Determining the absolute magnitude of hydrogen isotope effects. In *Isotope Effects on Enzyme-Catalyzed Reactions (Proceedings of the Sixth Annual Harry Steenbock Symposium)* (Cleland, W. W., O'Leary, M. H., and Northrop, D. B., Eds.) pp 122−152, University Park Press, Baltimore.
(40) Northrop, D. B. (1982) Deuterium and tritium kinetic isotope effects on initial rates. *Methods Enzymol. 87*, 607−625.
(41) Biemann, K. (1962) *Mass Spectrometry, Organic Chemical Applications*, McGraw-Hill, New York.
(42) Kuzmic, P. (1996) Program DYNAFIT for the analysis of enzyme kinetic data: Application to HIV protease. *Anal. Biochem. 237*, 260−273.
(43) Foust, G. P., Burleigh, B. D., Jr., Mayhew, S. G., Williams, C. H., Jr., and Massey, V. (1969) An anaerobic titration assembly for spectrophotometric use. *Anal. Biochem. 27*, 530−535.
(44) Burleigh, B. D., Jr., Foust, G. P., and Williams, C. H., Jr. (1969) A method for titrating oxygen-sensitive organic redox systems with reducing agents in solution. *Anal. Biochem. 27*, 536−544.
(45) Guengerich, F. P., and Johnson, W. W. (1997) Kinetics of ferric cytochrome P450 reduction by NADPH-cytochrome P450 reductase: Rapid reduction in the absence of substrate and variations among cytochrome P450 systems. *Biochemistry 36*, 14741−14750.
(46) Massey, V., and Hemmerich, P. (1977) A photochemical procedure for reduction of oxidation-reduction proteins employing deazariboflavin as catalyst. *J. Biol. Chem. 252*, 5612−5614.
(47) Hildebrandt, A. G., Roots, I., Tjoe, M., and Heinemeyer, G. (1978) Hydrogen peroxide in hepatic microsomes. *Methods Enzymol. 52*, 342−350.
(48) Gorsky, L. D., Koop, D. R., and Coon, M. J. (1984) On the stoichiometry of the oxidase and monooxygenase reactions catalyzed by liver microsomal cytochrome P-450: Products of oxygen reduction. *J. Biol. Chem. 259*, 6812−6817.
(49) Guengerich, F. P. (1983) Oxidation-reduction properties of rat liver cytochromes P-450 and NADPH-cytochrome P-450 reductase related to catalysis in reconstituted systems. *Biochemistry 22*, 2811−2820.
(50) O'Haver, T. C., and Green, G. L. (1976) Numerical error analysis of derivative spectrometry for the quantitative analysis of mixtures. *Anal. Chem. 48*, 312−318.
(51) Isin, E. M., and Guengerich, F. P. (2006) Kinetics and thermodynamics of ligand binding by cytochrome P450 3A4. *J. Biol. Chem. 281*, 9127−9136.
(52) Sohl, C. D., and Guengerich, F. P. (2010) Kinetic analysis of the three-step steroid aromatase reaction of human cytochrome P450 19A1. *J. Biol. Chem. 285*, 17734−17743.
(53) Griffin, B. W., and Peterson, J. A. (1972) Camphor binding by *Pseudomonas putida* cytochrome P-450. Kinetics and thermodynamics of the reaction. *Biochemistry 11*, 4740−4746.
(54) Cook, P. F., and Cleland, W. W. (2007) *Enzyme Kinetics and Mechanism*, Garland Science Publishing, New York.
(55) Cleland, W. W. (2005) The use of isotope effects to determine enzyme mechanisms. *Arch. Biochem. Biophys. 433*, 2−12.
(56) Miwa, G. T., and Lu, A. Y. H. (1987) Kinetic isotope effects and 'metabolic switching' in cytochrome P450-catalyzed reactions. *BioEssays 7*, 215−219.
(57) Jones, J. P., Korzekwa, K. R., Rettie, A. E., and Trager, W. F. (1986) Isotopically sensitive branching and its effect on the observed intramolecular isotope effects in cytochrome P-450 catalyzed reactions: A new method for the estimation of intrinsic isotope effects. *J. Am. Chem. Soc. 108*, 7074−7078.
(58) Jones, J. P., Rettie, A. E., and Trager, W. F. (1990) Intrinsic isotope effects suggest that the reaction coordinate symmetry for the cytochrome P-450 catalyzed hydroxylation of octane is isozyme independent. *J. Med. Chem. 33*, 1242−1246.
(59) Yun, C.-H., Miller, G. P., and Guengerich, F. P. (2001) Oxidations of *p*-alkoxyacylanilides catalyzed by human cytochrome P450 1A2: Structure-activity relationships and simulation of rate constants of individual steps in catalysis. *Biochemistry 40*, 4521−4530.
(60) Krauser, J. A., and Guengerich, F. P. (2005) Cytochrome P450 3A4-catalyzed testosterone 6β-hydroxylation stereochemistry, kinetic deuterium isotope effects, and rate-limiting steps. *J. Biol. Chem. 280*, 19496−19506.
(61) Sevrioukova, I. F., and Poulos, T. L. (2012) Structural and mechanistic insights into the interaction of cytochrome P450 3A4 with bromoergocryptine, a type I ligand. *J. Biol. Chem. 287*, 3510−3517.
(62) Sohl, C. D., Isin, E. M., Eoff, R. L., Marsch, G. A., Stec, D. F., and Guengerich, F. P. (2008) Cooperativity in oxidation reactions catalyzed by cytochrome P450 1A2: Highly cooperative pyrene hydroxylation and multiphasic kinetics of ligand binding. *J. Biol. Chem. 283*, 7293−7308.

(63) Ekroos, M., and Sjogren, T. (2006) Structural basis for ligand promiscuity in cytochrome P450 3A4. *Proc. Natl. Acad. Sci. U.S.A. 103*, 13682−13687.
(64) Yamazaki, H., Nakamura, M., Komatsu, T., Ohyama, K., Hatanaka, N., Asahi, S., Shimada, N., Guengerich, F. P., Shimada, T., Nakajima, M., and Yokoi, T. (2002) Roles of NADPH-P450 reductase and apo- and holo-cytochrome b_5 on xenobiotic oxidations catalyzed by 12 recombinant human cytochrome P450s expressed in membranes of *Escherichia coli*. *Protein Expression Purif. 24*, 329−337.
(65) Porubsky, P. R., Meneely, K. M., and Scott, E. E. (2008) Structures of human cytochrome P-450 2E1. Insights into the binding of inhibitors and both small molecular weight and fatty acid substrates. *J. Biol. Chem. 283*, 33698−33707.
(66) Yano, J. K., Hsu, M. H., Griffin, K. J., Stout, C. D., and Johnson, E. F. (2005) Structures of human microsomal cytochrome P450 2A6 complexed with coumarin and methoxsalen. *Nat. Struct. Biol. 12*, 822−823.
(67) Das, A., and Sligar, S. G. (2009) Modulation of the cytochrome P450 reductase redox potential by the phospholipid bilayer. *Biochemistry 48*, 12104−12112.
(68) Xiao, Y., Shinkyo, R., and Guengerich, F. P. (2011) Cytochrome P450 2S1 is reduced by NADPH-cytochrome P450 reductase. *Drug Metab. Dispos. 39*, 944−946.
(69) Song, W. C., and Brash, A. R. (1991) Purification of an allene oxide synthase and identification of the enzyme as a cytochrome-P-450. *Science 253*, 781−784.
(70) Björkhem, I. (1972) On the rate-limiting step in microsomal hydroxylation of steroids. *Eur. J. Biochem. 27*, 354−363.
(71) Björkhem, I. (1982) Rate limiting step in microsomal cytochrome P-450 catalyzed hydroxylations. In *Hepatic Cytochrome P-450 Monooxygenase System* (Schenkman, J. B., and Kupfer, D., Eds.) 1st ed., pp 645−666, Pergamon Press, New York.
(72) Gander, J. E., and Mannering, G. J. (1980) Kinetics of hepatic cytochrome P-450-dependent mono-oxygenase systems. *Pharmacol. Ther. 10*, 191−221.
(73) Ullrich, V. (1969) On the hydroxylation of cyclohexane in rat liver microsomes. *Hoppe-Seyler's Z. Physiol. Chem. 350*, 357−365.
(74) Bell-Parikh, L. C., and Guengerich, F. P. (1999) Kinetics of cytochrome P450 2E1-catalyzed oxidation of ethanol to acetic acid via acetaldehyde. *J. Biol. Chem. 274*, 23833−23840.
(75) Guengerich, F. P., Miller, G. P., Hanna, I. H., Sato, H., and Martin, M. V. (2002) Oxidation of methoxyphenethylamines by cytochrome P450 2D6. Analysis of rate-limiting steps. *J. Biol. Chem. 277*, 33711−33719.
(76) Cook, P. F. (1991) *Enzyme Mechanism from Isotope Effects*, 1st ed., CRC Press, Boca Raton, FL.
(77) Northrop, D. B. (1975) Steady-state analysis of kinetic isotope effects in enzymic reactions. *Biochemistry 14*, 2644−2651.
(78) Miwa, G. T., Walsh, J. S., and Lu, A. Y. H. (1984) Kinetic isotope effects on cytochrome P-450-catalyzed oxidation reactions: The oxidative O-dealkylation of 7-ethoxycoumarin. *J. Biol. Chem. 259*, 3000−3004.